Electronic Supplementary Material (ESI) for Materials Horizons.

Supporting Information

Low-damping Flexible $Y_3Fe_5O_{12}$ thin films for tunable RF/microwave processors

Yanan Zhao,[#a] *Yaojin Li,*[#a] *Ziyao Zhou,*[*a] *Renci Peng,*[a] *Shukai Zhu,*[a] *Mouteng Yao,*[a] *Bin Peng,*[a] *Yifan Zhao,*[a] *Yuxin Cheng,*[a] *Bian Tian,*[bc] *Zhongqiang Hu,*[a] *Zuo-Guang Ye,*[ad] *Zhuangde Jiang,*[bc] *and Ming Liu* [*ab]

a Electronic Materials Research Laboratory, Key Laboratory of the Ministry of Education, School of Electronic and Information Engineering, State Key Laboratory for Mechanical Behavior of Materials, Xi'an Jiaotong University, Xi'an 710049, China

E-mail: mingliu@xjtu.edu.cn, ziyaozhou@xjtu.edu.cn

b International Joint Laboratory for Micro/Nano Manufacturing and Measurement Technology, Xi'an Jiaotong University, Xi'an 710049, China

c State Key Laboratory for Manufacturing Systems Engineering, Xi'an Jiaotong University, Xi'an 710049, China

d Department of Chemistry and 4D LABS, Simon Fraser University, Burnaby, British Columbia V5A 1S6, Canada

#there authors contribute equally

Supplementary Note 1. The depositing process for the flexible YIG/Mica thin films

Figure S1 (a) shows the fabrication process of the highly flexible YIG thin films deposited on Mica substrates by the PLD technology, in which the Mica (thickness t = 10 μm) substrates became thin step by step through the mechanical exfoliation. The flexible YIG/Mica thin films not only keep the excellent magnetic properties but also have high flexibility suitable as RF/microwave materials, as shown in Figure S1 (b).

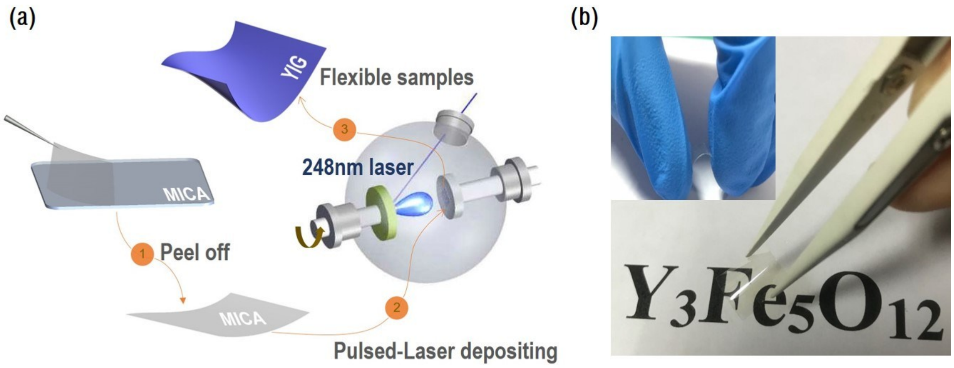

Supplementary Figure S1. (a) The schematic of the PLD process for the flexible YIG/Mica thin films. (b) The optical images of the flexible YIG/Mica thin films and Mica substrates, respectively.

Supplementary Note 2. The voltage tunability for the YIG/Mica/PMN-PT heterostructures

The voltage-tuning tendency for the low-damping YIG/Mica/PMN-PT heterostructures was also measured, as shown in Figure S2. A noticeable shift (95 Oe) of the in-plane FMR H_r field was obtained at the fixed electrostatic field of 8 kV·cm^{-1}, corresponding to a microwave ME coefficient of 12 Oe·cm·kV^{-1}. Meanwhile, a small shift (28.5 Oe) of the out-of-plane FMR H_r field was also observed when the magnetic field applied along the [011] direction of PMN-PT.

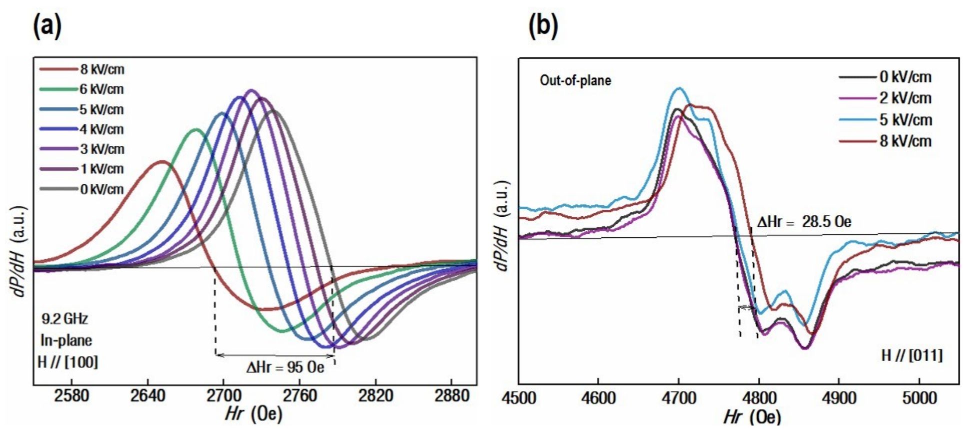

Supplementary Figure S2. (a) The FMR H_r shifts under the positive different electrostatic fields at 9.2 GHz, along the [100] direction of PMN-PT slabs. (b) The FMR H_r shifts under the positive different electrostatic fields at 9.2 GHz, along the [011] direction of PMN-PT slabs.

Supplementary Note 3. The tunable tendency in broadband FMR measurements for the flexible YIG/Mica thin films

We systematically tested and analyzed the shift trends of in-plane FMR H_r and f_r for the flexible YIG/Mica thin films by a homemade broadband system, and the results are shown in Supplementary Figure S3. When the static magnetic field is fixed at 2600 Oe, in-plane FMR f_r gradually decreases under the flexible compressive stress (Figure S3(c)) while increases under the flexible tensile stress (Supplementary Figure S3(d)). The broadband system has a lower sensitivity than the narrow-band measurement system (EPR). Therefore, the maximum variable quantity of in-plane FMR H_r and f_r may be somewhat different from that measured by the EPR system under the same flexible stress. But there does not affect the overall tunable trends.

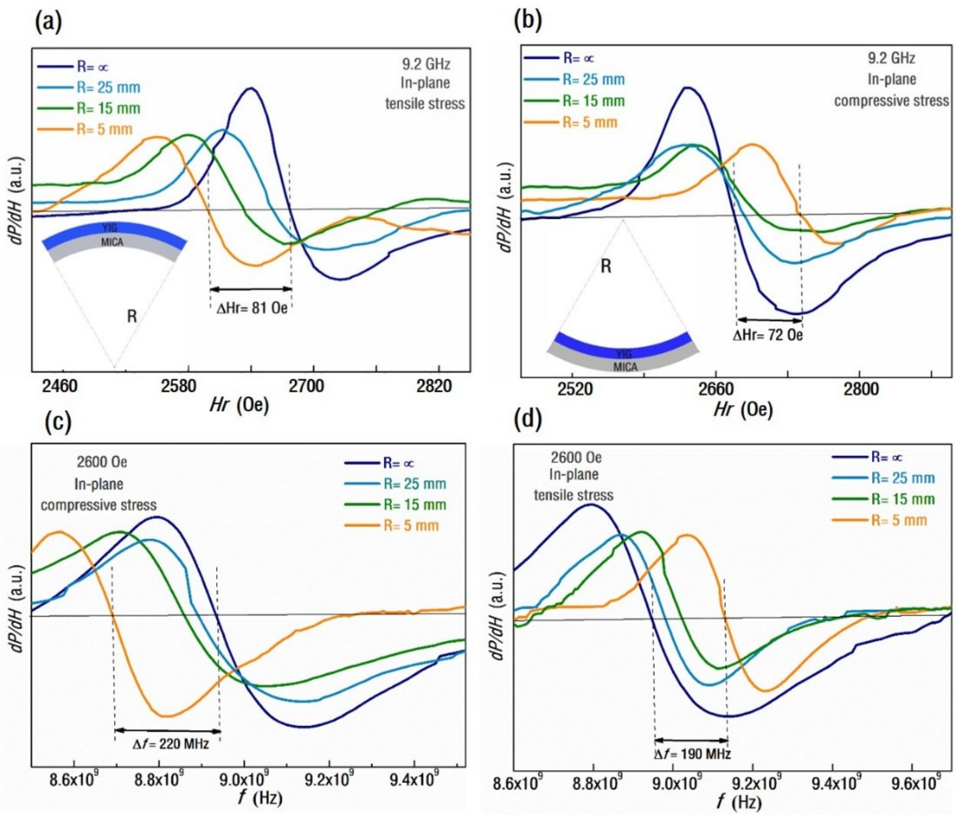

Supplementary Figure S3. The tunable tendency of in-plane FMR H_r spectra with different bending radii at 9.2 GHz, i.e., 5 mm (orange line), 15 mm (green line), 25 mm (cyan line) and flat state (dark blue line) under the flexible tensile (Figure S3(a)) and compressive stress (Figure S3(b)). The tunable tendency of in-plane FMR f_r spectra at 2600 Oe with different bending radii at 9.2 GHz, i.e., 5 mm (orange line), 15 mm (green line), 25 mm (cyan line) and flat state (dark blue line) under the flexible compressive (Figure S3(c)) and tensile stress (Figure S3(d)).

Supplementary Note 4. The *M-H* loops for the flexible YIG/Mica thin films

The magnetic hysteresis (*M-H*) loops of the flexible YIG/Mica thin film were also measured by a vibrating sample magnetometer (VSM) at room temperature, to investigate the tunable tendency of magnetic anisotropy induced by different flexible stresses. Figure S4 (a) shows a representative *M-H* loop for the flexible YIG/Mica thin films under the flat state, indicating a saturated magnetization (M_s) of 138.5 emu/cm^3 and a coercive field (H_c) of 20 Oe (in-plane direction). Because of the negative magnetostrictive coefficient of YIG, the magnetization became harder along the in-plane direction (parallel to the tensile stress direction) and became easier along the out-of-plane direction (vertical to the tensile stress direction), as shown in Figure S4 (b) and Figure S4 (c). In particular, the tuning shift of *M-H* loops is also remarkable along the out-of-plane direction, being consistent with that of out-of-plane FMR H_r fields.

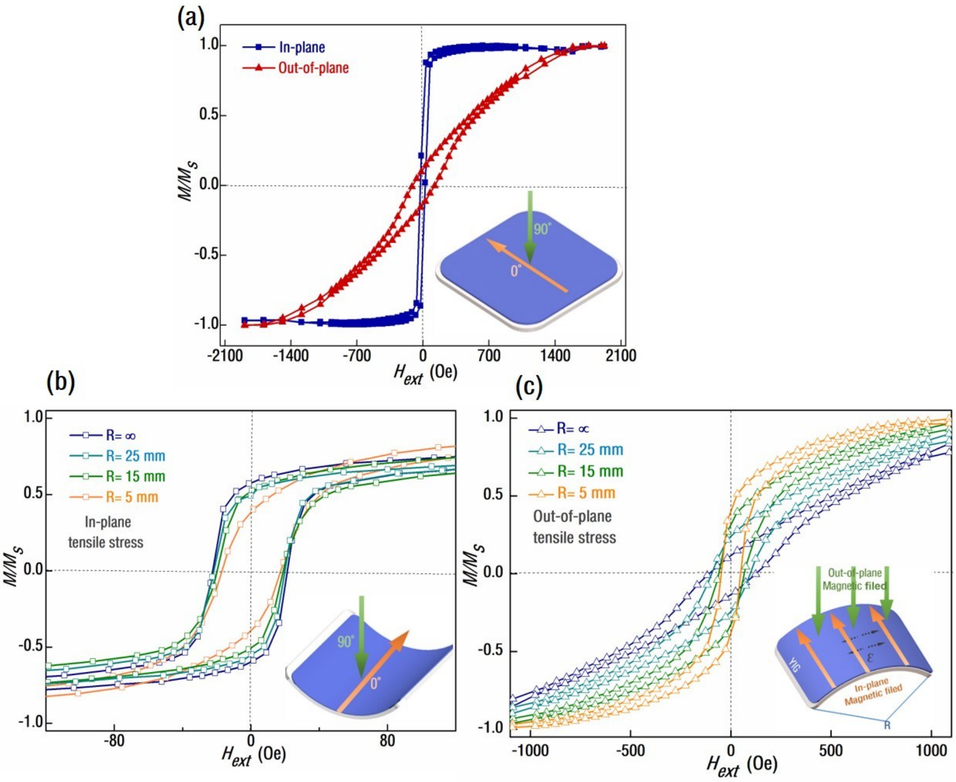

Supplementary Figure S4. (a) *M-H* loops under a flat state along the in-plane (dark blue line) and out-of-plane direction (red line). (b) *M-H* loops under flexible tensile stress along the in-plane direction, and out-of-plane direction (c) with different bending radii, i.e., 5 mm (orange line), 15 mm (green line), 25 mm (cyan line) and flat state (dark blue line).

Supplementary Note 5. The flexible integrated system for the YIG/Mica thin films

As shown in Figure S5, we also systematically tested and analyzed the tunable range of in-plane FMR H_r and f_r for the integrated, flexible devices designed with low-damping YIG thin films. It provides almost the same tunable value as that tested by the BBFMR system, as shown in Figure S3. Moreover, the flexible integrated system could also be used for the measurements of other flexible magnetic materials by modifying the flexible fixture.

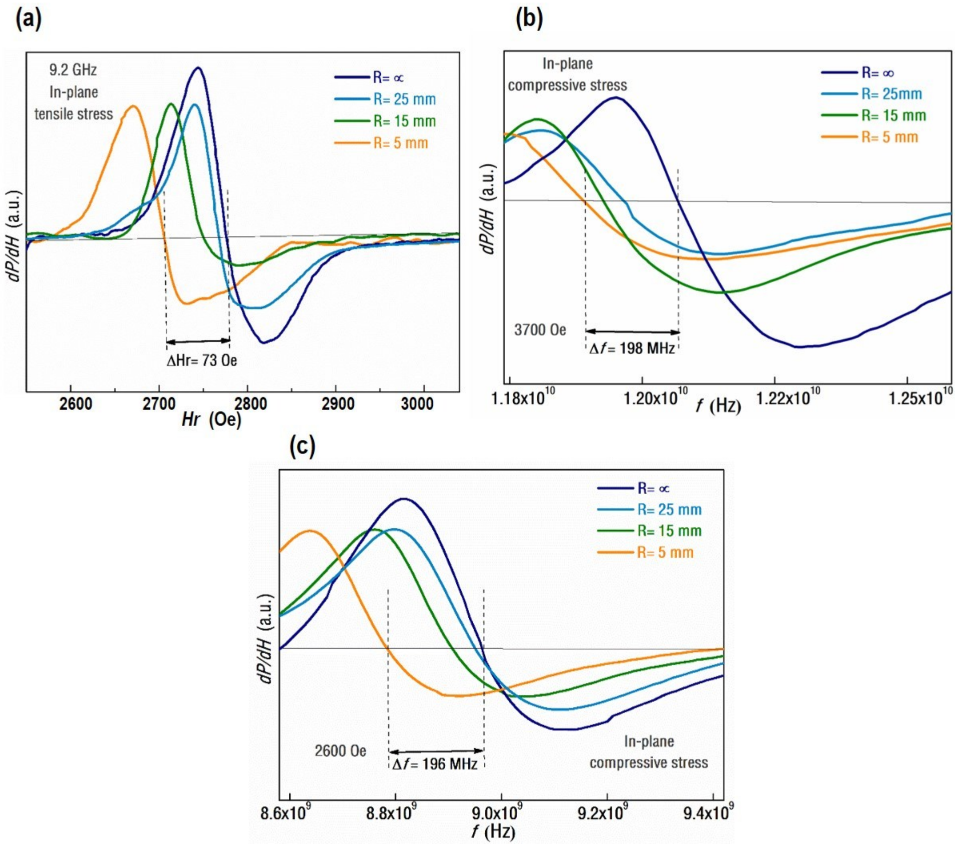

Supplementary Figure S5. (a) The in-plane FMR H_r spectra at 9.2 GHz with different flexible bending radii, i.e., 5 mm (orange line), 15 mm (green line), 25 mm (cyan line) and flat state (dark blue line). The shifts of the FMR f_r spectra at 3700 Oe (b) and 2600 Oe (c), respectively, measured by the flexible broadband system along the in-plane direction at different bending radii, i.e., 5 mm (orange line), 15 mm (green line), 25 mm (cyan line) and flat state (dark blue line) in the compressive stress state.

Supplementary Note 6. The stability and durability test for the flexible YIG/Mica thin films

Considering the practical application for the flexible YIG/Mica thin films, the stability and durability performance should be measured, as shown in Supplementary Figure S6. We also measured and compared the FMR spectra of the flexible YIG/Mica thin films respectively along the in-plane, 45˚, and out-of-plane directions, when under the initial and final states. The H_r and linewidth of the FMR spectra change little under repeated bending tests, showing an excellent fatigue-resistant behavior.

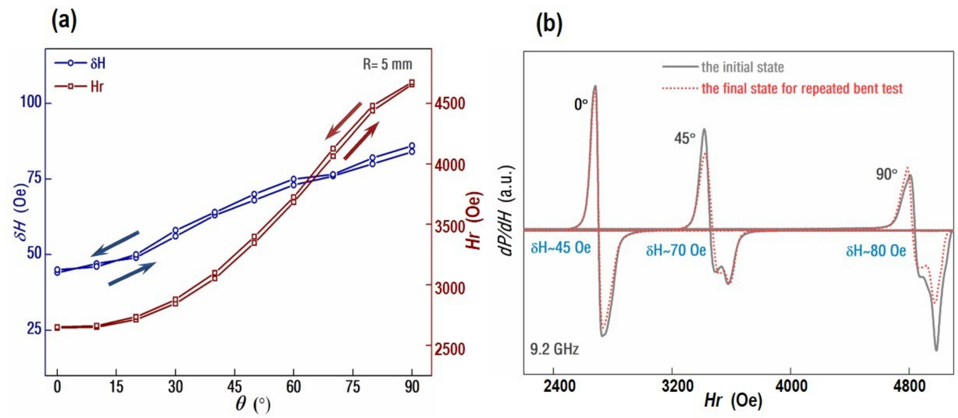

Supplementary Figure S6. (a) The comparison of H_r (red line) and linewidth (blue line) for the initial and final states, respectively, at the bending radius of 5 mm. (b)The comparison of the FMR spectra between the initial state (grey line) and the final state (red line) under the repeated bending tests.

Supplementary Note 7. The comparison of tunable ranges of FMR field in various YIG heterostructures.

The flexible tunability of flexible YIG film in our work, exhibit a large FMR tuning shift of 180 Oe/550 MHz along the out-of-plane direction, which is much larger than previous work.

Table 1. The comparative tunable range of FMR H_r or f_r for YIG

Samples	ΔH_r (Oe) or Δf_r (MHz) In-plane	ΔH_r (Oe) or Δf_r (MHz) Out-of-plane	E (kV/cm)	Bent radius	References
YIG(4.9 μm)/GGG/PMN-PT	44 Oe	18 Oe	8	——	1
YIG(10 μm)/GGG/PZT	122 MHz	——	5	——	2
YIG(100 μm)/GGG/PZN-PT	220 MHz	——	5	——	3
YIG(80 nm)/Mica/PMN-PT	95 Oe	28.5 Oe	8	——	Unpublished Our work
Flexible YIG(80 nm)/Mica	**89 Oe**	**180 Oe**	**——**	**5 mm**	**Our work**

	(225 MHz)	(550 MHz)			

Supplementary Note 8. The theoretical calculations for the flexible YIG/Mica thin films

8.1 The basic formula

Due to the effective demagnetizing factor[4] N_e induced by the change of the total energy density *E*, one can get a general basic formula for the ferromagnetic resonance (FMR)[4],

$$\frac{2\pi f}{\gamma} = \sqrt{(H_r + H_x)(H_r + H_y)} \tag{S1}$$

and[5] $H_i = N_e^i M_s$ with $i = \{x,y\}$ (S2)

Here, *i*=*x*, *i*=*y* mean the demagnetizing factors respectively stem from the *x*-*z* plane and *x*-*y* plane.

8.2 The effective demagnetizing factor

The signs of N_e are decided by the change tendency of the total energy density *E*, which is negative if the total energy density decreases while positive if the total energy density increases.

8.2.1 The flat thin films

The static magnetic field or the magnetization can rotate from the *z*-axis (out-of-plane direction) to the *x*-axis (in-plane direction) in the *x*-*z* plane, namely, from $\theta_0 = 0$ to $\theta_0 = \pi/2$. The change of the total energy density[4] in the *x*-*z* plane and the *x*-*y* plane respectively are,

$$\delta E_x = -\frac{K_u}{2}\left[cos^2(\epsilon + \theta_0) + cos^2(\epsilon - \theta_0)\right] + \frac{1}{4}\mu_0 M_S^2\left[cos^2(\epsilon + \theta_0) + cos^2(\epsilon - \theta_0)\right] \tag{S3}$$

$$\delta E_y = -K_u cos^2\epsilon cos^2\theta_0 + \frac{1}{2}\mu_0 M_S^2 cos^2\epsilon cos^2\theta_0 \tag{S4}$$

with the angle ϵ between the magnetization direction and the average magnetization direction, and the θ_0 is the angle between the normal direction and the average magnetization direction. Due to the equation[4] $\partial_\theta \delta E_i = \partial_\epsilon \delta E_i \approx N_e^i M_S^2 sin\epsilon$, the N_e^i can be described by

$$N_e^x = 2\frac{K_u}{M_S^2}cos2\theta_0 - \mu_0 cos2\theta_0 \tag{S5}$$

$$N_e^y = 2\frac{K_u}{M_S^2}cos^2\theta_0 - \mu_0 cos^2\theta_0 \tag{S6}$$

When $\theta_0 = 0$ (along the out-of-plane direction), $N_e^x = N_e^y = 2\frac{K_u}{M_S^2} - \mu_0$, while when $\theta_0 = \pi/2$ (along the in-plane direction), $N_e^x = -2\frac{K_u}{M_S^2} + \mu_0$ and $N_e^y = 0$.

8.2.2 The bending thin films

If the plane of the flexible film YIG/Mica thin films fixed in the *x*-*y* plane, the static magnetic field would rotate in the *y*-z plane, and the microwave field is along the *y*-axis. The total energy *E* is expressed as,

$$E = - K_u cos^2\theta + \frac{1}{2}\mu_0 M_S^2 cos^2\theta - \frac{1}{2}K_{2\perp}(\sigma)cos^2\theta - \frac{3}{2}\lambda_S\sigma^{\perp}cos^2\theta - \frac{3}{2}\lambda_S\sigma^{||}sin^2\theta cos^2\phi \tag{S7}$$

Where λ_S is the saturated magnetostrictive coefficient [1] of YIG (-2 ppm), $K_{2\perp}(\sigma)$ is the out-of-plane anisotropy induced by the flexible stress, and $\frac{3}{2}\lambda_S\sigma^{\perp}cos^2\theta$, $\frac{3}{2}\lambda_S\sigma^{||}sin^2\theta cos^2\phi$ respectively represent the effective magneto-elastic coupling interaction.

Case 1, Along the out-of-plane direction,

Because the static magnetic field will rotate in the *y-z* plane, here the azimuth $\phi = \frac{\pi}{2}$. In the-inclination direction and the-azimuth direction, one has respectively

$$\theta = \theta_0 \pm \epsilon \ and \ \phi = \phi_0 \tag{S8}$$

$$cos\theta = cos\theta_0 cos\epsilon \ and \ \phi = \phi_0 \pm arctan\frac{\epsilon}{sin\theta_0} \tag{S9}$$

by use of equation (S8) and (S9), one gets the effective demagnetizing factor N_e^i dependent on the equilibrium inclination θ_0 via the equation[4] $\partial_\theta \delta E_i = \partial_\epsilon \delta E_i \approx N_e^i M_S^2 sin\epsilon$,

$$N_e^x(\theta_0) = - 2\frac{K_{eff}}{M_S^2}cos2\theta_0 + 3\frac{\lambda_S\sigma^{\perp}}{M_S^2}cos2\theta_0 \tag{S10}$$

$$N_e^y(\theta_0) = -2\frac{K_{eff}}{M_S^2}cos^2\theta_0 + 3\frac{\lambda_S\sigma^{\perp}}{M_S^2}cos^2\theta_0 - 3\frac{\lambda_S\sigma^{||}}{M_S^2} \tag{S11}$$

$\theta_0 \in \left[-\frac{L}{2R},\frac{L}{2R}\right]$ with the bending radius R and the length L along the x-direction, and $K_{eff} = -K_u + \frac{1}{2}\mu_0 M_S^2 - \frac{1}{2}K_{2\perp}(\sigma)$. So average effective demagnetization factor N_e^i due to the change of the average total energy density can be adjusted as,

$$N_e^x = \frac{R}{L}\int_{-L/R/2}^{L/R/2} N_e^x(\theta_0)d\theta_0 = -2\frac{K_{eff}R}{M_S^2 L}sin\frac{L}{R} + 3\frac{\lambda_S}{M_S^2}\sigma^{\perp}(R)\frac{R}{L}sin\frac{L}{R} \tag{S12}$$

$$N_e^y = \frac{R}{L}\int_{-L/R/2}^{L/R/2} N_e^y(\theta_0)d\theta_0 = -\frac{K_{eff}}{M_S^2}\left(1 + \frac{R}{L}sin\frac{L}{R}\right) + \frac{3\lambda_S}{2M_S^2}\sigma^{\perp}(R)\left(1 + \frac{R}{L}sin\frac{L}{R}\right) \tag{S13}$$

Case 2, Along the in-plane direction,

When the static magnetic field is along the plane of flexible YIG/Mica thin films, in the case, the effective demagnetizing factors are simple and similar to that of the flat state applied by the stretching or electrostatic field.

$$N_e^z = 2\frac{K_{eff}}{M_S^2} - 3\frac{\lambda_S}{M_S^2}\sigma^{\perp} \tag{S14}$$

$$N_e^y = -3\frac{\lambda_S}{M_S^2}\sigma^{||} \tag{S15}$$

In conclusion, synthetically considering the effective demagnetizing factor N_e and the flexible stress, the in-plane FMR frequency formula should be adjusted as,

$$\frac{2\pi f}{\gamma} = \sqrt{\left(H_r + 2\frac{K_{eff}}{M_s} - 3\frac{\lambda_S}{M_S^2}\sigma^{\perp}\right)\left(H_r - 3\frac{\lambda_S}{M_S^2}\sigma^{||}\right)} \tag{S16}$$

and for the out-of-plane direction,

$$\frac{2\pi f}{\gamma} = \sqrt{\left(H_r + (-2\frac{K_{eff}}{M_s} + 3\frac{\lambda_S\sigma^{\perp}}{M_s})f_x(R)\right)\left(H_r + \left(-2\frac{K_{eff}}{M_S^2} + 3\frac{\lambda_S\sigma^{\perp}}{M_S^2}\right)f_y(R) - 3\frac{\lambda_S}{M_s}\sigma^{||}\right)} \tag{S17}$$

where $f_x^{out} = \frac{R}{L}sin\frac{L}{R}$, and $f_y^{out}(R) = (1 + \frac{R}{L}sin\frac{L}{R})/2$ are the flexible tuning factors, due to the non-uniform angle between the magnetization direction and the normal direction for the out-of-plane direction. The FMR frequency of the flexible YIG/Mica thin films could be reset back to the initial flat state of $R \to \infty$, as shown in Figure S6 (a), so the flexible stress should only come from the bending of thin films and be expressed as $\sigma \propto 1/R$.

8.3 The discussion of theoretical simulation

Here, the out-of-plane anisotropy $K_{2\perp}(\sigma)$ induced by the flexible stress/strain is proportional to L/R, which the corresponding effective field is $H_{2\perp}(\sigma) = H_{2\perp} * \frac{L}{R}$ with the first parameter $H_{2\perp}$. The magneto-elastic anisotropy induced by the flexible stress is also considered for the flexible YIG thin films, in which the $H_{\sigma,out}^{ave} = 135.8$ Oe and $H_{\sigma,in}^{ave} = 340$ Oe is within the appropriate ratio range (1/2~1/3) that the ratio of along the out-of-plane to the in-plane direction. However, Mica is an ideal substrate for van der Waals (vdW) heteroepitaxy. Hence, the orientation of YIG thin films grown on Mica substrates depends on the current growth parameters and Mica surface state, which is consistent with the growth of YIG along (531) orientation rather than on along Mica (001) orientation in our research. For simplicity, we will introduce two parameters proportional to 1 / R to evaluate $\sigma^{\perp}$ and $\sigma^{||}$. However, it is noted that the ratio is suitable even if the effective fields may be smaller than that of simulation calculation. Based on the above considerations, there was a simple relation between $H_{eff}^{\sigma^{\perp}}(R) = 3\frac{\lambda_S}{M_s}\sigma^{\perp}(R)$ and $H_{eff}^{\sigma^{||}}(R) = 3\frac{\lambda_S}{M_s}\sigma^{||}(R)$, $H_{eff}^{\sigma^{||}}(R) = H_{eff}^{\sigma^{\perp}}(R) * \frac{H_{\sigma,in}^{ave}}{H_{\sigma,out}^{ave}}$.

Given the $H_{eff}^{\sigma^{\perp}}(R) = H_{eff}^{out} * \frac{L}{R}$ with the second parameter H_{eff}^{out}, the fitting results are shown in Figure S7, in which the values of fitting parameters are $H_{2\perp} = 25.5\ Oe$ and $H_{eff}^{out} = 40.3\ Oe$.

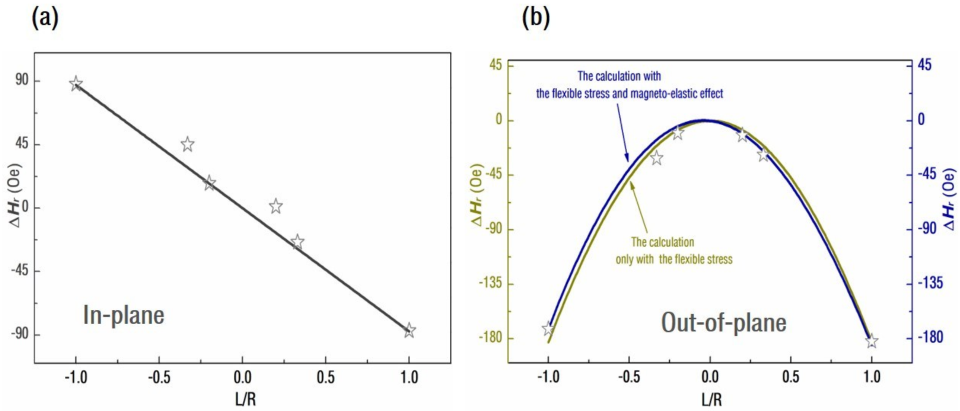

Supplementary Figure S7. (a) The fitted results of the in-plane FMR H_r field under different flexible stresses. (b) The revised fitted results of out-of-plane FMR filed with flexible tunable factors under different flexible stresses.

From the tunable tendency of the in-plane FMR H_r field, the contributions of the flexible stress, the stretching or electric field are the same. When along the out-of-plane direction, there is a large shift than that of the in-plane FMR H_r field, and the tuning tendency is the same under any flexible stress. But there should be a small shift induced by magneto-elastic anisotropy fields than that of the in-plane FMR H_r field. The flexible tunable factors, $f_x(R) = \frac{R}{L} sin\frac{L}{R}$ and $f_y(R) = (1 + \frac{R}{L} sin\frac{L}{R})/2$ are introduced to explain the change for the out-of-plane FMR field, which has a symmetrical tuning and distinct shift, as shown in Figure S7 (b). Therefore, there will be a symmetrical tune and greater change with the smaller effective field, because the flexible tuning factors are symmetry and global of R

In addition, the simulation results are $H_{2\perp}$= 0 Oe and H_{eff}^{out}= 0 Oe, in which there is no contribution induced by the magneto-elastic anisotropy field. It indicates a very remarkable tuning of the out-of-plane FMR field even just the bending of flexible magnetic thin films.

References

1. S. Shastry, G. Srinivasan, M. I. Bichurin, V. M. Petrov and A. S. Tatarenko, *Physical Review B*, 2004, **70**, 064416-064416.
2. I. V. Zavislyak, M. A. Popov, G. Sreenivasulu and G. Srinivasan, *Appl. Phys. Lett.*, 2013, **102**, 222407.

3. J. L. Guo-Min Yang, Jing Wu, Ming Liu, Geyi Wen, Yaqiu Jin and Nian X. Sun, *IEEE MTT-S International Microwave Symposium*, 2011, 4.
4. C. Kittel, *Physical Review*, 1948, **73**, 155-161.
5. D. L. M. Rodrigo Arias, *Physical Review B*, 1999, **60**, 6.